

# Erosion-corrosion of RAFM JLF-1 steel in Lithium flow induced by impeller

M. Kondo<sup>1</sup>, V. Tsisar<sup>2</sup>, T. Muroga<sup>1</sup>, T. Nagasaka<sup>1</sup>, O. Yeliseyeva<sup>2</sup>

<sup>1</sup>*Fusion Engineering Research Center, National Institute for Fusion Science, Toki, Japan*

<sup>2</sup>*Physical-Mechanical Institute of National Academy of Sciences of Ukraine, L'viv, Ukraine*

(Received: 26 October 2009 / Accepted: 9 March 2010)

The purpose of the present study is to investigate erosion-corrosion characteristics of reduced activation ferritic martensitic steel, JLF-1 (Fe-9Cr-2W) in flowing Li. The erosion-corrosion characteristics were investigated by means of corrosion tests with rectangular plate type specimen of JLF-1 in Li stirring pot, where the Li flow was induced by impeller in the pot. The test temperature was 500°C and 600°C, and there was no temperature difference in the Li stirring pot. The erosion-corrosion characteristics were evaluated by the weight loss measurement of the specimens and metallurgical analysis for the corroded surface. The results were compared with those obtained from the tests at static condition to feature the effect of Li flow on the corrosion. The weight loss of the specimens tested in Li flow was larger than that tested in the static tests. The corroded surface showed the local corrosion along lath boundary and grain boundary of JLF-1 as the same as that after the test at static condition. There were defects which were not observed in the specimen tested at the static condition. The defects were the trace of the erosion-corrosion. The corrosion attack to the boundaries made weak bonding between the subgrains, and the subgrains were peeled from the surface by the Li flow.

Keywords: Corrosion, Erosion, Erosion-corrosion, Lithium, Blanket, RAFM

## 1. Introduction

Blanket concepts with liquid metal lithium (Li) breeder/coolant provide attractive options for high tritium breeding ratio, high efficiency and simplicity of the system [1]. Fe-Cr-W based RAFM (Reduced Activation Ferritic/Martensitic) steels are widely regarded as promising structural materials of the blanket system, because of its low activation properties, radiation resistance and industrial maturity. JLF-1 (Japanese Low activation Ferritic steel 1, Fe-9Cr-2W) has excellent resistance against neutron irradiation in both microstructural and mechanical properties [2], and is a potential candidate for the structural material of blanket.

The corrosion characteristics of JLF-1 in Li have been investigated by authors. The authors found that the JLF-1 showed phase transformation from martensite to ferrite due to the carbon depletion from the steel surface in Li [3]. It was found that the phase transformation was caused by the low carbon potential in Li [4]. The carbide in the grain boundary, block boundary and lath boundary was dissolved by the Li. These boundaries were selectively corroded. Cr in the steel matrix was also depleted by the Li with nitrogen via the formation of unstable nitride of Li-N-Cr [5].

The corrosion test at flowing condition is necessary to investigate the effect of mass transfer on the corrosion [6]. The corrosion test by thermal convection Li loop has been performed to investigate the mass transfer due to the temperature difference in the system. In the convection Li loop, the flow velocity was small, i.e. 5cm/s, and the effect of the shear stress by the flow on the corrosion is small [7].

The erosion-corrosion in flowing lead-bismuth (Pb-Bi) at high flow velocity of 2m/s was reported in ref. [8]. The corroded surface was mechanically eroded by the high density fluid flow. However, the data of erosion-corrosion by liquid Li was limited.

The stirred pot type corrosion test apparatus was developed to investigate the effect of mass transfer and shear stress by the Li flow on the corrosion. The Li flow was induced by the circulating impeller. There was no temperature difference in the Li. The corrosion tests by the stirred pot were performed and the corrosion characteristics were compared with that obtained from the test at static condition. The purpose of the present study is to investigate the erosion-corrosion characteristics in the Li flow induced by impeller.

## 2. Experimental condition

### 2.1 Experimental apparatus

The static test was performed using the test apparatus shown in Fig. 1. The detail was described in the previous reports of ref. [3, 4 and 9]

The stirred pot (Fig. 2) was designed to investigate the effect of flow conditions on the corrosion without temperature gradient. The higher flow velocity than that in thermal convection loop can be given in the test. The pot was assembled in glove box as the same as the test in Li pot. The specimens were fixed using the specimen holder as the same as the simple immersion. The crucible made of 9Cr steel was used in place of Mo crucible, though the Mo was more corrosion resistant than the Fe-9Cr in the Li. The Mo crucible was not used to remove the effect of carbon trapping on the corrosion and some precipitation of Mo dissolved in flowing Li on the

author's e-mail: kondo.masatoshi@nifs.ac.jp

weight loss measurement for specimens [4, 6 and 9].

The flow of Li in the pot was induced by rotating impeller. The baffle plate for decrease the rotating flow was not placed in the pot, and the pot was so-called unbaffled stirred pot [10]. The rotating flow with small upward and down ward flow of Li was made by the rotating impeller. Then, the Li was mixed well and the concentration of impurity between upper part and lower one became the same. The flow velocity was roughly estimated as inertial Li flow as the flow velocity became the same to the speed of impeller. The velocity is obtained by the following equation of

$$V_{Li} = \pi dn \quad (1)$$

where  $V_{Li}$  is flow velocity on the specimen surface in unit of m/s,  $d$  is width of impeller in unit of m and  $n$  is rotating speed in unit of  $s^{-1}$ . The width of impeller  $d$  was 0.033m and the rotating speed was 100rpm, which corresponded to  $1.66s^{-1}$  in the present work. Then, the flow velocity on the specimen surface was estimated as 0.17m/s. Reynolds number for mixing in the pot was estimated by

$$Re_{mixing} = \frac{\rho nd^2}{\mu} \quad (2)$$

where  $\rho$  is the density of Li in unit of  $kg/m^3$  and  $\mu$  is viscosity of Li in unit of Pa s. The data for thermal properties of liquid Li were obtained in ref. [11]. Reynolds number was 2538 at  $500^\circ C$  and 2859 at  $600^\circ C$ , this indicates that the flow in the pot was possibly turbulent flow. The flowing condition was determined due to the investigation on the erosion-corrosion characteristics of JLF-1 steels in flowing Li with higher shear stress on the surface at turbulent flow conditions.

## 2.2 Experimental condition

Chemical component of JLF-1 (JOYO-HEAT) is 8.93Cr- 0.49Ni- 1.96W- 0.64Mn- 0.21V- 0.01C- 0.015N- Fe balanced. The size of specimen was 10mm x 15mm x 2mm. The specimens were heat-treated at  $1050^\circ C$  /3.6ks/air cooled (normalizing) and  $780^\circ C$  /3.6 ks/air cooled (tempering). The specimens were polished to remove the native oxide layer and then cleaned in the acetone and ethanol. The surface was mechanically polished using SiC papers grit order: 180→400/P800→800/P1200 followed by finishing with alumina with particle size  $0.3\mu m$  and  $0.05\mu m$ .

The experimental conditions are presented in Table 1. The ratio of the volume of Li to specimen surface area was almost the same, though the volume of Li and the specimen number were different in each test.

After the corrosion test, specimens were taken out from Li, and the adhered Li was removed in water.

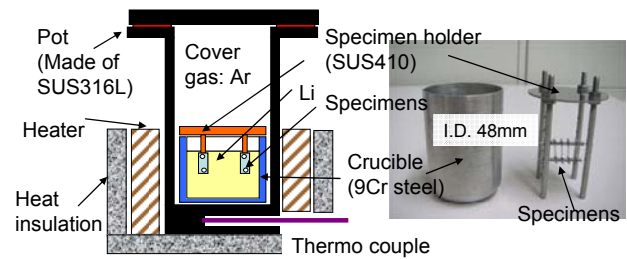


Fig. 1 Static test pot

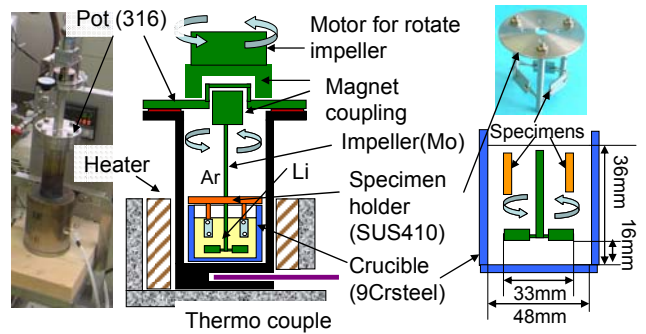


Fig. 2 Stirring Li test pot

The nitrogen content in Li was analyzed before and after the corrosion tests by ammonia extraction titration method to check the increase of the nitrogen content. The analysis results indicated no change of nitrogen content in Li by the test. The weight change of the specimens before and after the test was measured using electro reading balance with the accuracy of 0.1mg.

The corroded surface was analyzed by using scanning electron microscope and energy dispersive x-ray spectroscopy (SEM/EDX). The initial surface of the specimen was analyzed by SEM/EDX after the electro etching at 30V in the pool of 13% $HClO_4$ - 13% Ethyleneglycol monobutyl ether – 10% ethanol- 64% acetic acid. The other specimen was analyzed by SEM/EDX without etching procedure after the test.

## 3. Results and Discussion

### 3.1 Weight loss of the specimens

The results of weight loss measurement are shown in Fig.3. In the static tests, the weight loss was larger at higher temperature. This indicated the corrosion was larger at higher temperature. In the tests at  $500^\circ C$ , the loss and scattering was larger at the flowing condition than that at static condition at  $500^\circ C$ . The scattering of the weight loss data was large not only after the corrosion test but flowing test at  $600^\circ C$ .

The larger weight loss by the Li flow was due to (1) accelerated dissolution of steel alloying elements by mass transfer in Li flow and (2) effect of mechanical shear stress on the surface by the flow.

Table 1 Corrosion test conditions

	Temp. (°C)	Time (hour)	Volume of Li (cc)	Flow velocity on specimen surface (m/s)	Nitrogen content in Li (wppm)	Specimen number	Li volume /surface area [m]
Test at static condition	500	283	80	0	65	3	0.008
	600 [4]	250	92	0	65	10	0.007
Test in stirred condition	500	250	65	0.17	65	3	0.008
	600	250	65	0.17	65	3	0.008

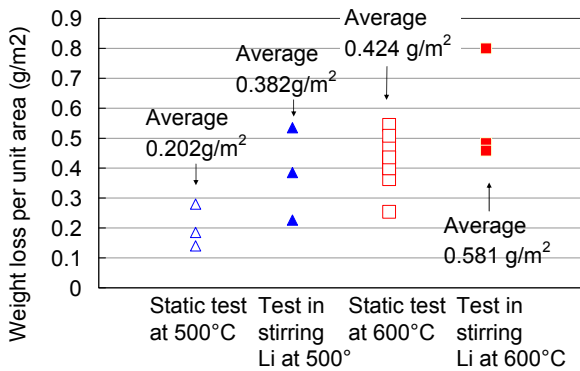


Fig. 3 Weight loss of specimen by corrosion in Li at static and stirring condition

3.2 Observation of corroded surface

Fig. 4 shows the SEM image of specimen

surface before and after the corrosion tests, and Table 2 presents the chemical components of surface analyzed by EDS. The specimen surfaces before the corrosion test (Fig.4 (a)) showed precipitated carbides on the surface, and the carbides outlined the boundaries. The boundaries were grain boundary, block boundary and lath boundary.

In the static test at 500°C (Fig.4 (b)), the carbide was not observed though the surface showed martensite structure. There was gap along the boundaries. This gas might be caused by the dissolution of carbides Li. After the static tests at 600°C, the clear boundary of ferrite was observed due to the phase transformation in Li by carbon depletion as reported in ref. [3, 4] (Fig.4 (c)). The precipitated carbide was dissolved by Li and the Li penetrated into the grain boundary.

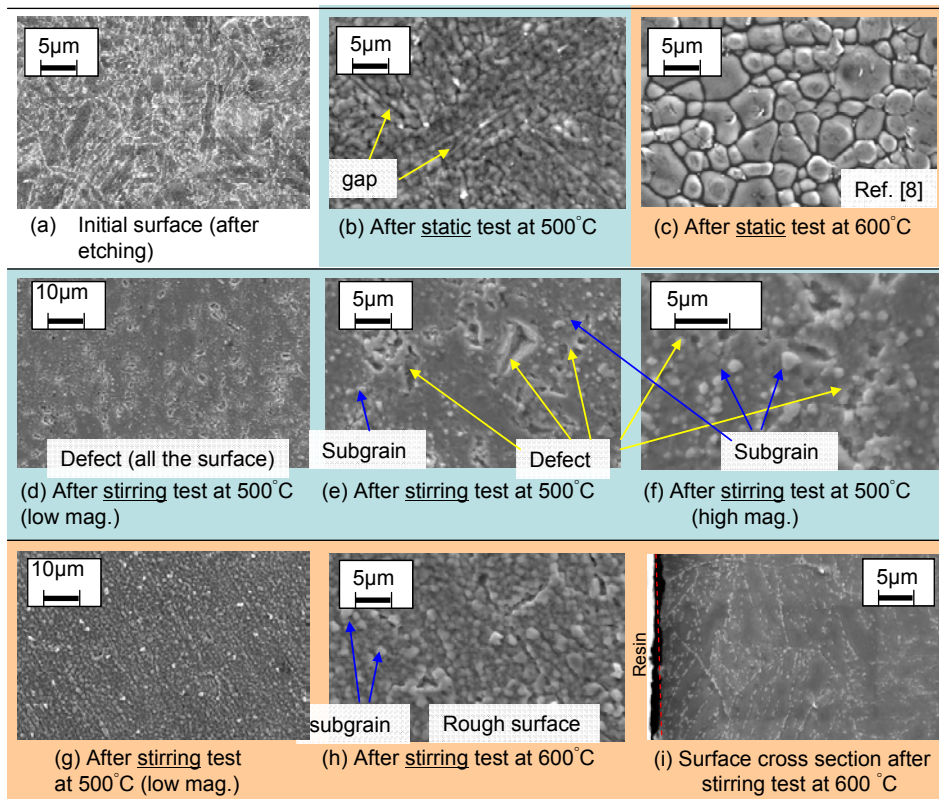


Fig.4 Corroded surface (a) initial surface after etching, (b) after static test at 500°C, (c) after static test at 600°C (d) after stirring test at 500°C, (e) defect after stirring test at 500°C, (f) after stirring test at 500°C(high magnification), (g) after stirring test at 600°C (low mag.), (h) rough surface after stirring test at 600°C and (i) surface cross section after stirring test at 600°C (electro etching)

Table 2 Chemical composition of surface analyzed by EDX after corrosion test (wt%)

Temperature	Condition	Chemical composition		
		Cr	W	Fe
Initial steel		8.9	2.0	
500	Static	8.8	2.0	Balance
	Stirring	7.2	1.1	
600	Static	7.9	2.0	Balance
	Stirring	6.4	1.1	

The surface after the test in stirring Li at 500°C showed small grains and defects (Figs.4 (d) to (f)), which were not detected in the static test (Fig. 4 (b)). The size of small grains was less than 1µm, and these small grains might be martensite lath subgrains [12]. The size of the defects was 1-5µm. The defects were possible due to the depletion of subgrains in the stirring Li. The EDX analysis showed the depletion of W, which was not caused in static Li. Phase transformation from martensite to ferrite was not observed after the test in static and flowing Li at 600°C.

Large number of the subgrains was observed on the specimen surface after the test in stirring Li at 600°C. The defects, which were observed after the test in stirring Li at 500°C, were not clearly detected. The phase transformation was not detected after the test in flowing Li at 600°C. The EDX analysis for the surface indicated that the depletion of

Cr and W from the surface by the corrosion. The result of surface cross sectional analysis after electro etching procedure was shown in Fig. 4 (i). The loss of the carbides on the surface as reported in [3,4 and 9] was not observed.

### 3.3 Erosion-corrosion mechanism

The mechanism of erosion-corrosion in stirring Li is summarized in Fig. 5 based on the experimental results. The Li attacked to the boundary of subgrains, though the Li was not detected because the penetrated Li was removed in the cleaning procedure of the specimens. In the same time, the carbides were dissolved by the Li. By the penetration of the Li to the boundary, the bonding between the subgrains became weak. The shear stress and/or normal stress, which worked on the steel surface, peeled off the subgrains. The defects shown in Figs. 4 (d-f) were the trace of the erosion-corrosion in Li. The rough surface shown in Figs.4 (g, h) is caused by the erosion-corrosion, which was more severe than that at 500°C.

The corrosion in static Li may promote the coarsening of the subgrains. Fig. 4(c) showed larger size of the grains. On the contrary, the coarsening was not observed after the test at flowing condition. The subgrains were peeled off by the Li flow, and then, the subgrains were not able to be coarsened.

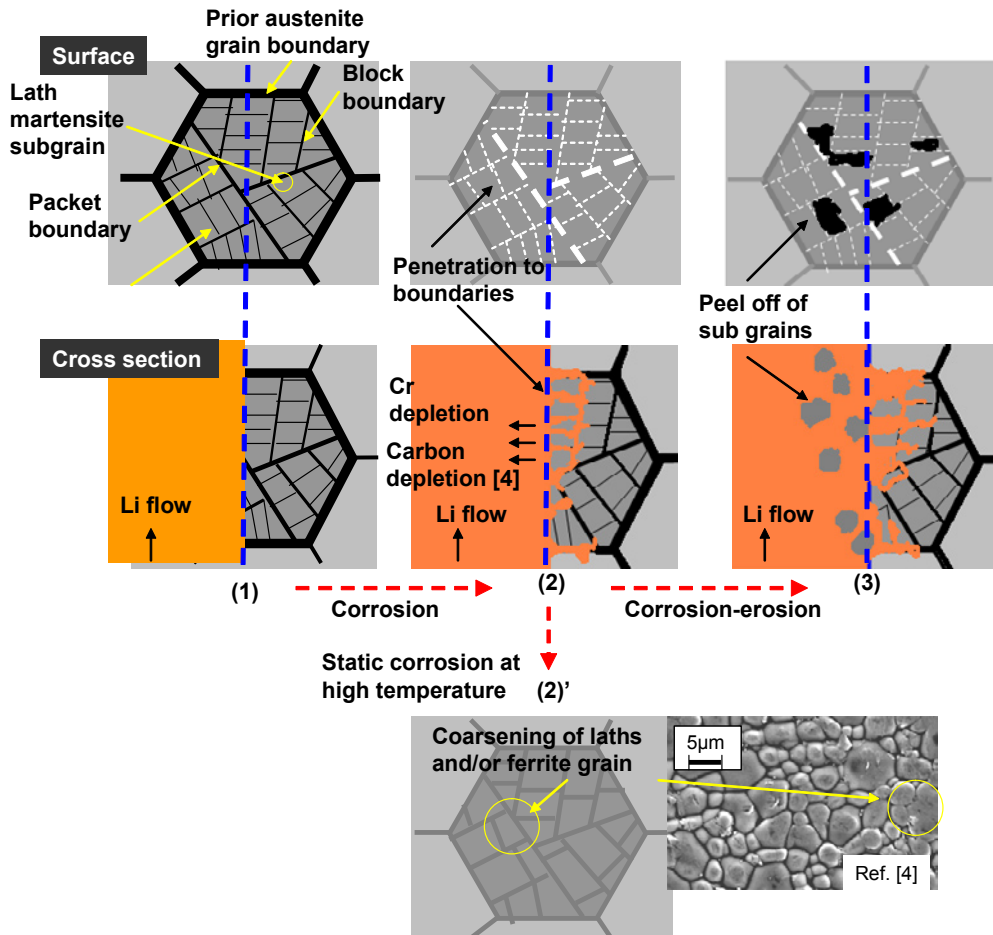


Fig. 5 Mechanism of erosion-corrosion in stirring Li and coarsening of subgrain in static corrosion

### 3.4 Mass transfer

The corrosion of steels in the stirring Li was caused by mass transfer. The corrosion was caused by the Cr depletion as mentioned in previous chapter. Therefore, the mass transfer of Cr was discussed here. The concentration difference of Cr in the boundary layer on the steel surface was assumed to be the model of the mass transfer. Then, the mass flux from the steel to Li,  $J$  in unit of  $\text{g/m}^2\text{s}$  in the corrosion is expressed as

$$J = h_{D,s}\rho(C_s - C) \quad (3)$$

where  $h_{D,s}$  is coefficient for mass transfer in unit of  $\text{m/s}$ ,  $\rho$  is density of Li with dissolved steel element in unit of  $\text{g/m}^3$ ,  $C_s$  is the solubility of dissolved element in weight ratio,  $C$  is the concentration of dissolved element in Li in weight ratio.

The information for the solubility of Cr in Li is limited. The solubility was evaluated from the weight losses of specimens in the previous static tests, which shows the parabolic rate law and constant weight loss after 250 hours test [3, 4]. The solubility was determined as 48wppm at  $500^\circ\text{C}$  and 96wppm at  $600^\circ\text{C}$ . The solubility at  $500^\circ\text{C}$  was slightly higher than that in literature data (26wppm) at  $523^\circ\text{C}$  [13] because the solubility included the dissolution of other metal such as Fe and W.

The transient of concentration of Cr in Li by the corrosion is expressed as

$$\rho V \frac{dC}{dt} = JS \quad (4)$$

where  $V$  is the volume of Li in unit of  $\text{m}^3$  and  $S$  is total surface area of specimens. The corrosion of inner surface crucible made of 9Cr steel was taken into account as the same dissolution per unit area might be caused as the specimen. The equation for the concentration is obtained by eqs. (3) and (4) using the boundary condition  $t=0$  and  $C=0$  as

$$C = C_s \left(1 - \exp\left(-\frac{h_{D,static} St}{V}\right)\right) \quad (5)$$

where  $t$  is the exposure time in unit of  $\text{s}$ , Then, the mass balance between the weight loss of specimens and the increase of Cr concentration in Li is given from eq. (5) as

$$\Delta m = \rho V C_s \left(1 - \exp\left(-\frac{h_{D,static} St}{V}\right)\right) \quad (6)$$

where  $\Delta m$  is the total weight loss of all specimens in unit of  $\text{g}$ .

The coefficient of mass transfer was determined by Sherwood number and Schmidt number as

$$\text{Sh} = \frac{h_{D,m} d}{D_{me}} = K(\text{Re}_{\text{mixing}})^{2/3} (\text{Sc})^{1/3} \quad (7)$$

$$\text{Sc} = \frac{\nu}{D_{Cr}} \quad (8)$$

where  $K$  is coefficient depends on the shape of impeller and varied between 0.6 to 0.3 [14].  $K$  was selected as 0.35 from the empirical data, which was correlated with the ratio of inner diameter of crucible to the width of impeller.  $\nu$  is kinematic viscosity of Li at  $500^\circ\text{C}$  in unit of  $\text{m}^2/\text{s}$ ,  $D_{Cr}$  is diffusion coefficient of Cr in Li at  $500^\circ\text{C}$ . The data of  $D_{Cr}$   $2.20 \times 10^{-8} \text{m}^2/\text{s}$  at  $570^\circ\text{C}$  [13] was used for the evaluation of  $500^\circ\text{C}$  and  $600^\circ\text{C}$ .  $\text{Sc}$  number was 32.5 at  $500^\circ\text{C}$  and 28.9 at  $600^\circ\text{C}$ .  $\text{Sh}$  number was 207 at  $500^\circ\text{C}$  and 200 at  $600^\circ\text{C}$ . Then,  $h_{D, \text{mixing}}$  was obtained as  $1.39 \times 10^{-4} \text{m/s}$  at  $500^\circ\text{C}$  and  $1.33 \times 10^{-4} \text{m/s}$  at  $600^\circ\text{C}$ .

The weight loss of specimens for 250 hours exposure was obtained by eq. (7) using the above mentioned mass transfer coefficient. The effect of the corrosion of crucible made of Fe-9Cr steel was taken into account for the estimation based on the assumption the corrosion loss of the Fe-9Cr was the same to that of JLF-1 specimens. The specimen loss theoretically obtained from eq. (6) was estimated as  $0.178 \text{g/m}^2$  at  $500^\circ\text{C}$  and  $0.349 \text{g/m}^2$  at  $600^\circ\text{C}$ .

The averaged weight loss of the steel in the static Li was  $0.202$  at  $500^\circ\text{C}$  and  $0.424 \text{g/m}^2$  at  $600^\circ\text{C}$ . The averaged weight loss of the steel in the stirring Li flow was  $0.382$  at  $500^\circ\text{C}$  and  $0.581 \text{g/m}^2$  at  $600^\circ\text{C}$ . The weight loss data obtained by the corrosion experiment at static condition was slightly larger than that of theoretical value. The saturation of the Cr in the Li [13] was indicated even at the static condition. The weight loss at flowing condition was larger than that of theoretical value. The reason was the erosion-corrosion, which was caused by physical stress of Li flow.

In the case of erosion-corrosion of steels in the flowing Pb-Bi [8], the weight loss was much larger than that without erosion occurrence. That was because of continuous corrosion occurrence without the saturation in the non-isothermal flowing system, and the erosion was continuously caused by the corrosion. Further study is necessary for the detail estimation of erosion-corrosion in the Li flow using non-isothermal flowing system.

#### 4. Conclusion

Erosion-corrosion characteristics of JLF-1 steel (Fe-9Cr-2W) in flowing Li without temperature difference was investigated by means of corrosion experiment using stirring Li pot. The results were compared with that of static tests to feature the effect of Li flow. Major conclusions are follows;

- (1) The weight loss of the specimens tested in flowing Li was larger than that in static Li at the same temperature because of mass transfer and erosion corrosion.
- (2) The corroded surface was partly eroded in stirring Li flow at 500°C.
- (3) The specimen surface had large number of small grains after the corrosion test in flowing Li at 600°C. The grains might be martensite lath subgrain. The boundary of subgrains was clearly revealed because of the corrosion. The erosion-corrosion was caused by that the peeling off of the subgrains from the steel matrix by the Li flow.
- (4) The weight loss obtained in the corrosion experiment in flowing Li was larger than that evaluated by the mass transfer equation. The difference between the experimental data and theoretical evaluation was due to the erosion-corrosion.
- (5) The erosion-corrosion was controlled by the suppression of corrosion due to the saturation of dissolved alloying elements from the steel into the Li at isothermal Li system.

#### 5. Acknowledgement

This work was supported by NIFS budget code NIFS08UCFF004 NIFS09UCFF004 and Grant-in-Aid for Scientific Research (A) 19206100 (2007-2009).

#### 6. References

- [1] T. Muroga, M. Gasparotto, Fusion Eng. Design 61-62 (2002) 13-25.
- [2] A. Kohyama, T. Kohno, K. Asakura, H. Kayano, J. Nucl. Mater., 212-215 (1994) 684-689.
- [3] Qi Xu, Masatoshi Kondo, Takuya Nagasaka, Takeo Muroga, Masaru Nagura, Akihiro Suzuki, Fusion Eng. Design, 83 (2008) 1477-1483.
- [4] Q. Xu, M. Kondo et al., Effect of Chemical Potential of Carbon on Phase Transformation and Corrosion of JLF-1 Steel in a Static Lithium, J. Nucl. Mater, 394, 20-25, (2009).
- [5] V. Tsisar, M. Kondo, Q. Xu, T. Muroga, T. Nagasaka, O. Yeliseyeva, Effect of nitrogen on the corrosion behavior of RAFM, JLF-1 steel in Lithium, in proceeding of ICFRM-14, (2009).
- [6] M. Kondo, T. Muroga, Q. Xu, V. Tsisar, T. Nagasaka, T. Oshima, Mass transfer of RAFM steel in Li by simple immersion, impeller induced flow and thermal convection, in proceeding of ICFRM-14 (2009).
- [7] P. F. Tortorelli, Journal of Nuclear Materials, 722-727, 155-157 (1988).

- [8] M. Kondo, M. Takahashi, T. Suzuki, K. Ishikawa, K. Hata, S. Qiu and H. Sekimoto, J. Nucl. Mater., 343, 349-359 (2005).
- [9] Q. Xu, Doctorate thesis, Department of Fusion Science, The Graduate University for Advanced Studies (2008).
- [10] T.R. Cumby, J. Agric. Engng Res, 45, 157-173 (1990).
- [11] JSME Data Book : Heat transfer 4<sup>th</sup> edition, Maruzen corp. *in Japanese* (1991).
- [12] F. Abe, T. Noda and M. Okada, J. Nucl. Mater., 195, 51-62 (1992).
- [13] G.M. Griaznov, V.A. Evtikhin, L.P. Zavialskiy et al., Interaction of structural materials with liquid metals under the isothermal conditions, in: Material science of liquid metal systems of thermonuclear reactors, *in Russia* Moscow, Energoatomizdat, 1989, pp. 32-142.
- [14] Chemical engineering, kagakukougakkai, *in Japanese* (1992).